Periodica Polytechnica
Mechanical Engineering

59(2), pp. 65-73, 2015
DOI: 10.3311/PPme.7153
Creative Commons Attribution

RESEARCH ARTICLE

Elastic Analysis of Rotating Thick Cylindrical Pressure Vessels under Non-Uniform Pressure: Linear and Non-Linear Thickness

Mohammad Zamani Nejad[1 *], Mehdi Jabbari[1], Mehdi Ghannad[2]

Received 06 November 2013; accepted after revision 27 January 2015

Abstract

Using multi-layers method (MLM), a semi-analytical solution have been derived for determination of displacements and stresses in a thick cylindrical shell with variable thickness under non-uniform pressure. Three different profiles (convex, linear and concave) are considered for the variable thickness cylinder. Given the existence of shear stress in the thick cylindrical shell due to thickness and pressure changes along the axial direction, the governing equations are obtained based on first-order shear deformation theory (FSDT). These equations are in the form of a set of general differential equations with variable coefficients. Given that the thick cylinder with variable thickness is divided into n homogenous disks, n sets of differential equations with constant coefficients are obtained. The solution of this set of equations, applying the boundary conditions and continuity conditions between the layers, yields displacements and stresses. Finally, some numerical results are presented to study the effects of applied pressure, thickness profile type, and angular velocity on the mechanical behavior of the cylindrical shell.

Keywords

rotating thick cylindrical shell, variable thickness, hyperbolic profile, non-uniform pressure, multi-layers method (MLM)

[1] Mechanical Engineering Department, Yasouj University
Yasouj 75914-353, Iran

[2] Mechanical Engineering Faculty, Shahrood University, Shahrood, Iran

[*] Corresponding author, e-mail: m.zamani.n@gmail.com, m_zamani@yu.ac.ir

1 Introduction

Thick cylindrical shells with variable thickness have widely been applied in many fields such as space fight, rocket, aviation, and submarine technology [15]. Given the limitations of the classic theories of thick wall shells, very little attention has been paid to the analytical and semi-analytical solutions of these shells [16]. Assuming the transverse shear effect, Naghdi and Cooper [12], formulated the theory of shear deformation. The solution of thick cylindrical shells of homogenous and isotropic materials, using the first-order shear deformation theory (FSDT) derived by Mirsky and Hermann [11]. Greenspon [7], opted to make a comparison between the findings regarding the different solutions obtained for cylindrical shells. A paper was also published by Kang and Leissa [8], where equations of motion and energy functionals were derived for a three-dimensional coordinate system. Eipakchi et al. [3] used the FSDT in order to derive governing equations of the thick cylinders with varying thickness and solved the equations using perturbation theory. Kang [9] used tensor calculus to derive a complete set of three-dimensional field equations well-suited for determining the behavior of thick shells of revolution having arbitrary curvature and variable thickness. Duan and Koh [2] derived an analytical solution for axisymmetric transverse vibration of cylindrical shells with thickness varying monotonically in arbitrary power form due to forces acting in the transverse direction, in terms of generalized hypergeometric function.

The field equations are utilized to express them in terms of displacement components. Using tensor analysis, a complete 3-D set of field equations developed for elastic analysis of thick shells of revolution with arbitrary curvature and variable thickness along the meridional direction made of functionally graded materials by Nejad et al. [17]. Ghannad et al. [4], making use of the FSDT obtained analytical solution for homogeneous and isotropic truncated thick conical shell. Ghannad and Nejad [5], obtained the differential equations governing the homogenous and isotropic axisymmetric thick-walled cylinders with same boundary conditions at the two ends were generally derived, making use of FSDT and the virtual work principle. Following that, the set of non-homogenous linear differential equations for the cylinder with

clamped-clamped ends was solved. A rotating variable-thickness heterogeneous elastic cylinder containing a fiber-reinforced viscoelastic core of uniform thickness is analytically studied by Zenkour [19]. He assumed the thickness and elastic properties of the external cylinder to be functions of the radial coordinate.

More recently, Kang [10] presented a 3-D method of analysis for determining the free vibration frequencies of joined thick conical-cylindrical shells of revolution with variable thickness. An analytical solution for clamped-clamped thick cylindrical shells with variable thickness subjected to constant internal pressure are presented by Ghannad et al. [6]. Nejad et al. obtained an analytical solution for stresses and radial displacement of homogeneous [13] and axially functionally graded material [14] rotating thick cylindrical shells with variable thickness using FSDT and multi-layers method (MLM).

In this paper, an elastic analysis has been presented for rotating cylindrical shell with variable thickness under non-uniform pressure. Thickness variation of the cylinder in axial direction is described by means of hyperbolic function. The governing equations have been derived, which in the axisymmetric condition and elasto-static state are a system of ordinary differential equations with variable coefficients. These equations normally do not have exact solutions. The MLM is used in order to solve the system of equations with variable coefficients. For this purpose, a rotating cylindrical shell with variable thickness is divided into homogenous disks. With regard to the continuity between layers and applying boundary conditions, the governing set of differential equations with constant coefficients is solved. The results obtained for stresses and displacements are compared with the solutions carried out through the finite element method (FEM). Good agreement is found between the results.

2 Problem formulation

In FSDT, the sections that are straight and perpendicular to the mid-plane remain straight but not necessarily perpendicular after deformation and loading. In this case, shear strain and shear stress are taken into consideration. Geometry of a thick cylindrical shell with variable thickness h, and the length L, is shown in Fig. 1. The clamped-clamped cylinder with variable thickness is subjected to non-uniform internal pressure P. The cylinder is rotating around its axis with constant angular velocity ω.

The location of any typical point m, within the shell element may be determined by R and z, as

$$\begin{cases} m:(r,x), \quad r = R + z \\ -\dfrac{h}{2} \le z \le \dfrac{h}{2} \quad \& \quad 0 \le x \le L \end{cases} \tag{1}$$

where z is the distance of typical point from the middle surface. In Eq. (1), R and variable thickness h are

$$\begin{cases} R = \dfrac{R_o + R_i}{2} \\ h = R_o - R_i \end{cases} \tag{2}$$

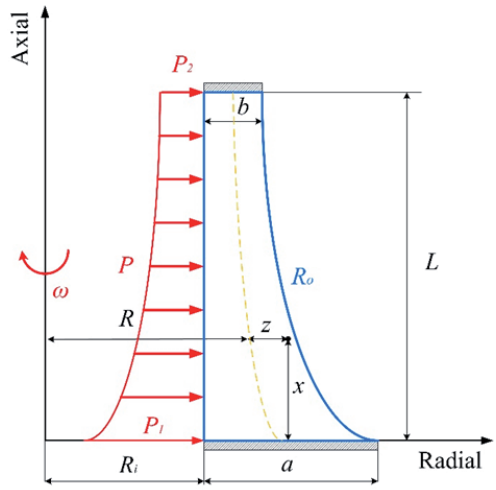

Fig. 1 Thick cylindrical shell with variable thickness

where R_0 is outer diameter function as

$$R_o = R_i + a - (a - b)\left(\frac{x}{L}\right)^{m_g} \tag{3}$$

Here m_g is geometric parameter such that $m_g > 0$. A cylinder with uniform thickness disk can be obtained from Eq. (3) by setting $m_g = 1$. The profile is concave if $m_g < 1$ and it is convex if $m_g > 1$. (See Fig. 2)

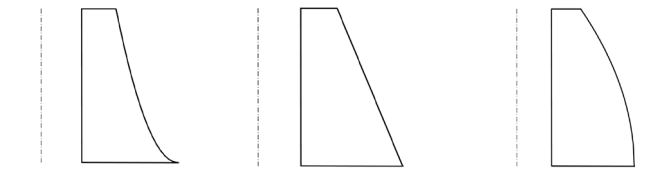

(a) concave ($m_g < 1$) (b) linear ($m_g = 1$) (c) convex ($m_g > 1$)

Fig. 2 Thickness profiles of thick cylindrical shell

The general axisymmetric displacement field (U_x , U_z), in the FSDT could be expressed on the basis of axial and radial displacements, as follows

$$\begin{Bmatrix} U_x \\ U_z \end{Bmatrix} = \begin{Bmatrix} u(x) \\ w(x) \end{Bmatrix} + \begin{Bmatrix} \phi(x) \\ \psi(x) \end{Bmatrix} z \tag{4}$$

where u (x) and w (x) are the displacement components of the middle surface. Also, ϕ (x) and ψ (x) are the functions of displacement field. The strain-displacement relations in the cylindrical coordinates system are

$$\begin{cases} \varepsilon_x = \dfrac{\partial U_x}{\partial x} = \dfrac{du}{dx} + \dfrac{d\phi}{dx} z \\ \varepsilon_\theta = \dfrac{U_z}{r} = \dfrac{1}{R+z}(w + \psi z) \\ \varepsilon_z = \dfrac{\partial U_z}{\partial z} = \psi \\ \gamma_{xz} = \dfrac{\partial U_x}{\partial z} + \dfrac{\partial U_z}{\partial x} = \left(\phi + \dfrac{dw}{dx}\right) + \dfrac{d\psi}{dx} z \end{cases} \tag{5}$$

The stresses on the basis of constitutive equations for non-homogenous and isotropic materials are as follows

$$\begin{cases} \sigma_i = \lambda\left[(1-\nu)\varepsilon_i + \nu\left(\varepsilon_j + \varepsilon_k\right)\right] \quad , \quad i \neq j \neq k \\ \tau_{xz} = \lambda\left[(1-2\nu)\dfrac{\gamma_{xz}}{2}\right] \quad , \quad \lambda = \dfrac{E}{(1+\nu)(1-2\nu)} \end{cases} \tag{6}$$

where σ_i and ε_i are the stresses and strains in the axial (x), tangential (θ), and radial (z) directions. The normal forces (N_x, N_θ, N_z), shear force (Q_x), bending moments (M_x, M_θ, M_z), and the torsional moment (M_{xz}), in terms of stress resultants are

$$\begin{Bmatrix} N_x \\ N_\theta \\ N_z \end{Bmatrix} = \int_{-h/2}^{h/2} \begin{Bmatrix} \sigma_x\left(1+\dfrac{z}{R}\right) \\ \sigma_\theta \\ \sigma_z\left(1+\dfrac{z}{R}\right) \end{Bmatrix} dz \tag{7}$$

$$\begin{Bmatrix} M_x \\ M_\theta \\ M_z \end{Bmatrix} = \int_{-h/2}^{h/2} \begin{Bmatrix} \sigma_x\left(1+\dfrac{z}{R}\right) \\ \sigma_\theta \\ \sigma_z\left(1+\dfrac{z}{R}\right) \end{Bmatrix} z dz \tag{8}$$

$$Q_x = K\int_{-h/2}^{h/2} \tau_{xz}\left(1+\frac{z}{R}\right)dz \tag{9}$$

$$M_{xz} = K\int_{-h/2}^{h/2} \tau_{xz}\left(1+\frac{z}{R}\right)z dz \tag{10}$$

where K is the shear correction factor that is embedded in the shear stress term. In the static state, for cylindrical shells K = 5/6 [18]. On the basis of the principle of virtual work, the variations of strain energy are equal to the variations of the external work as follows

$$\delta U = \delta W \tag{11}$$

where U is the total strain energy of the elastic body and W is the total external work due to internal pressure. The strain energy is

$$\begin{cases} U = \iiint_V U^* dV \\ dV = r dr d\theta dx = (R+z) dx d\theta dz \\ U^* = \dfrac{1}{2}\left(\sigma_x\varepsilon_x + \sigma_\theta\varepsilon_\theta + \sigma_z\varepsilon_z + \tau_{xz}\gamma_{xz}\right) \end{cases} \tag{12}$$

The variation of the strain energy is

$$\delta U = \int_0^{2\pi}\int_0^L\int_{-h/2}^{h/2} \delta U^*(R+z)\, dz dx d\theta \tag{13}$$

The resulting Eq. (13) will be

$$\frac{\delta U}{2\pi} = \int_0^L\int_{-h/2}^{h/2} \begin{bmatrix} \sigma_x \\ \sigma_\theta \\ \sigma_z \\ \tau_{xz} \end{bmatrix} \begin{bmatrix} \delta\varepsilon_x & \delta\varepsilon_\theta & \delta\varepsilon_z & \delta\gamma_{xz} \end{bmatrix} (R+z)\, dz dx \tag{14}$$

The external work is

$$\begin{cases} W = \iint_S \left(\vec{f}_{sf}\cdot\vec{u}\right)dS + \iiint_V \left(\vec{f}_{bf}\cdot\vec{u}\right)dV \\ dS = r_i d\theta dx = \left(R - \dfrac{h}{2}\right)d\theta dx \\ \vec{f}_{sf}.\vec{u} = -PU_z \\ \vec{f}_{bf}.\vec{u} = -\rho\omega^2(R+z)U_z \end{cases} \tag{15}$$

For axial distribution of inner pressure, the model of Eq. (16) is selected.

$$P = P_1 + \left(P_2 - P_1\right)\left(\frac{x}{L}\right)^{m_p} \tag{16}$$

Here P_1 and P_2 are the values of pressure at the $x = 0$ and $x = L$, respectively. m_p is constant parameter that is used to control the pressure profile. Thus the variation of the external work is as follows

$$\begin{aligned} \delta W = &\int_0^{2\pi}\int_0^L \left(P\delta U_z\right)\left(R - \frac{h}{2}\right)dx d\theta \\ &- \int_0^{2\pi}\int_0^L\int_{-h/2}^{h/2} \rho\omega^2\left(R+z\right)^2 \delta U_z dz dx d\theta \end{aligned} \tag{17}$$

The resulting Eq. (17) will be

$$\begin{aligned} \frac{\delta W}{2\pi} = &\int_0^L P\delta U_z\left(R - \frac{h}{2}\right)dx \\ &- \int_0^L\int_{-h/2}^{h/2} \rho\omega^2\left(R+z\right)^2 \delta U_z dz dx \end{aligned} \tag{18}$$

Substituting Eqs. (14) and (18) into Eq. (11), and drawing upon the calculus of variation and the virtual work principle, with regard to Eqs. (7-10), we will have:

$$\begin{cases} R\dfrac{dN_x}{dx} = 0 \\ \dfrac{d}{dx}\left(RM_x\right) - RQ_x = 0 \\ \dfrac{d}{dx}\left(RQ_x\right) - N_\theta = -P\left(R - \dfrac{h}{2}\right) - \dfrac{\rho\omega^2}{6}\dfrac{h}{2}\left(12R^2 + h^2\right) \\ \dfrac{d}{dx}\left(RM_{xz}\right) - M_\theta - RN_z = P\dfrac{h}{2}\left(R - \dfrac{h}{2}\right) - \dfrac{\rho\omega^2}{6}Rh^3 \end{cases} \tag{19}$$

and the boundary conditions at the two ends of the cylinder are

$$R\left[N_x\delta u+M_x\delta\phi+Q_x\delta w+M_{xz}\delta\psi\right]_0^L=0 \tag{20}$$

In order to solve Eq. (19), forces and moments need to be expressed in terms of the components of displacement field, using Eq. (6). Thus, Eq. (19) could be derived as follows

$$\begin{cases}[B_1]\dfrac{d^2}{dx^2}\{y\}+[B_2]\dfrac{d}{dx}\{y\}+[B_3]\{y\}=\{F\}\\ \{y\}=\{(du/dx)\quad \phi\quad w\quad \psi\}^T\end{cases} \tag{21}$$

The coefficients matrices $[B_i]_{4\times4}$, and force vector $\{F\}_{4\times1}$ are as follows

$$[B_1]=\begin{bmatrix}0 & 0 & 0 & 0\\ 0 & (1-\nu)\dfrac{h^3}{12}R & 0 & 0\\ 0 & 0 & \mu hR & \dfrac{\mu h^3}{12}\\ 0 & 0 & \dfrac{\mu h^3}{12} & \dfrac{\mu h^3}{12}R\end{bmatrix} \tag{22}$$

$$[B_2]=\begin{bmatrix}0 & (1-\nu)\dfrac{h^3}{12} & 0 & 0\\ (1-\nu)\dfrac{h^3}{12} & (1-\nu)\dfrac{h^2}{12}\left(3R\dfrac{dh}{dx}+h\dfrac{dR}{dx}\right) & -\mu hR & -(\mu-2\nu)\dfrac{h^3}{12}\\ 0 & \mu hR & \mu\left(R\dfrac{dh}{dx}+h\dfrac{dR}{dx}\right) & \dfrac{\mu h^2}{4}\dfrac{dh}{dx}\\ 0 & (\mu-2\nu)\dfrac{h^3}{12} & \dfrac{\mu h^2}{4}\dfrac{dh}{dx} & \dfrac{\mu h^2}{12}\left(3R\dfrac{dh}{dx}+h\dfrac{dR}{dx}\right)\end{bmatrix} \tag{23}$$

$$[B_3]=\begin{bmatrix}(1-\nu)hR & 0 & \nu h & \nu hR\\ (1-\nu)\dfrac{h^2}{4}\dfrac{dh}{dx} & -\mu hR & 0 & \dfrac{\nu h^2}{2}\dfrac{dh}{dx}\\ -\nu h & \mu\left(R\dfrac{dh}{dx}+h\dfrac{dR}{dx}\right) & -(1-\nu)\alpha & -h+(1-\nu)\alpha R\\ -\nu hR & \dfrac{\mu h^2}{4}\dfrac{dh}{dx} & -h+(1-\nu)\alpha R & -(1-\nu)\alpha R^2\end{bmatrix} \tag{24}$$

$$\{F\}=\frac{1}{\lambda}\begin{Bmatrix}C_0\\ 0\\ -P\left(R-\dfrac{h}{2}\right)-\dfrac{\rho\omega^2}{6}\dfrac{h}{2}\left(12R^2+h^2\right)\\ P\dfrac{h}{2}\left(R-\dfrac{h}{2}\right)-\dfrac{\rho\omega^2}{6}Rh^3\end{Bmatrix} \tag{25}$$

where the parameters are as follows

$$\begin{cases}\mu=\dfrac{5}{12}(1-2\nu)\\ \alpha=\ln\left(\dfrac{R+h/2}{R-h/2}\right)\end{cases} \tag{26}$$

3 Multi-layered method

Eq. (21) is the set of non-homogenous linear differential equations with variable coefficients. An analytical solution of this set of differential equations with variable coefficients seems to be difficult, if not impossible, to obtain. Hence, in the current study, a semi-analytical method for the solution of Eq. (21) is presented.

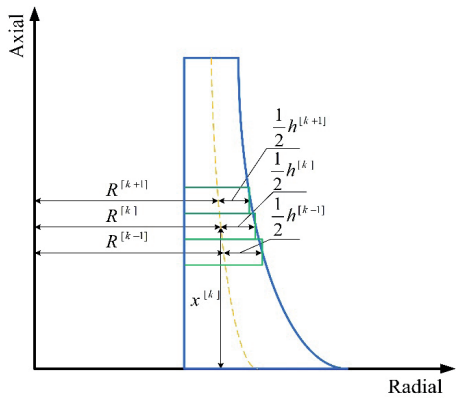

Fig. 3 Division of the cylinder with hyperbolic thickness into disks with constant thickness

In MLM, a cylinder with variable thickness is divided into homogenous disk layers with constant thickness $h^{[k]}$ (Fig. 3). Therefore, the governing equations convert to a nonhomogeneous set of differential equations with constant coefficients. $x^{[k]}$ and $R^{[k]}$ are length and radius of the middle of disks. k is the corresponding number given to each disk and n_d is the number of disks. The length of middle $x^{[k]}$ of kth disk (see Fig. 4) is as follows. The radius of middle point of each disk is as follows

$$\begin{cases}R^{[k]}=\dfrac{R_o^{[k]}+R_i}{2}\\ h^{[k]}=R_o^{[k]}-R_i\end{cases} \tag{27}$$

where

$$R_o^{[k]}=R_i+a-(a-b)\left(\frac{x^{[k]}}{L}\right)^{m_g} \tag{28}$$

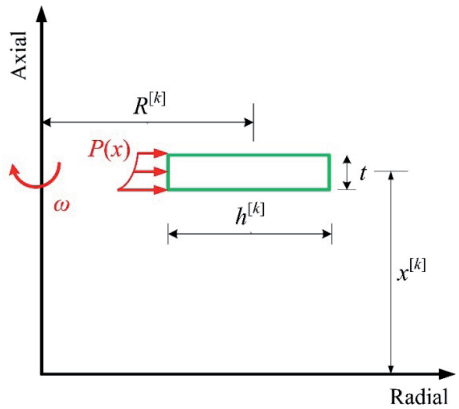

Fig. 4 Geometry of an arbitrary homogenous disk layer

Thus,

$$\left(\frac{dh}{dx}\right)^{[k]} = 2\left(\frac{dR}{dx}\right)^{[k]} = \left(\frac{dR_o}{dx}\right)^{[k]} \tag{29}$$

where

$$\left(\frac{dR_o}{dx}\right)^{[k]} = -m_g\left(\frac{a-b}{L}\right)\left(\frac{x^{[k]}}{L}\right)^{m_g-1} \tag{30}$$

With considering shear stress and based on FSDT, nonhomogeneous set of ordinary differential equations with constant coefficient of each disk is obtained.

$$\begin{cases} [B_1]^{[k]}\dfrac{d^2}{dx^2}\{y\}^{[k]} + [B_2]^{[k]}\dfrac{d}{dx}\{y\}^{[k]} + [B_3]^{[k]}\{y\}^{[k]} = \{F\}^{[k]} \\ \{y\}^{[k]} = \left\{(du/dx)^{[k]} \quad \phi^{[k]} \quad w^{[k]} \quad \psi^{[k]}\right\}^T \end{cases} \tag{31}$$

Defining the differential operator $P(D)$, Eq. (31) is written as

$$\begin{cases} \left[P(D)\right]^{[k]} = [B_1]^{[k]}D^2 + [B_2]^{[k]}D + [B_3]^{[k]} \\ D^2 = \dfrac{d^2}{dx^2} \quad , \quad D = \dfrac{d}{dx} \end{cases} \tag{32}$$

Thus

$$\left[P(D)\right]^{[k]}\{y\}^{[k]} = \{F\}^{[k]} \tag{33}$$

The above differential Equation has the total solution including general solution for homogeneous case $\{y\}_h^{[k]}$ and particular solution $\{y\}_p^{[k]}$, as follows:

$$\{y\}^{[k]} = \{y\}_h^{[k]} + \{y\}_p^{[k]} \tag{34}$$

For the general solution for homogeneous case, $\{y\}_h^{[k]} = \{V\}^{[k]}e^{m^{[k]}x}$ is substituted in $\left[P(D)\right]^{[k]}\{y\}^{[k]} = 0$. Thus

$$\begin{vmatrix} B_{11}^{[k]} & B_{12}^{[k]} & B_{13}^{[k]} & B_{14}^{[k]} \\ B_{21}^{[k]} & B_{22}^{[k]} & B_{23}^{[k]} & B_{24}^{[k]} \\ B_{31}^{[k]} & B_{32}^{[k]} & B_{33}^{[k]} & B_{34}^{[k]} \\ B_{41}^{[k]} & B_{42}^{[k]} & B_{43}^{[k]} & B_{44}^{[k]} \end{vmatrix} = 0 \tag{35}$$

where

$$B_{11}^{[k]} = (1-\nu)h^{[k]}R^{[k]} \tag{36}$$

$$B_{12}^{[k]} = m(1-\nu)\frac{\left(h^{[k]}\right)^3}{12} \tag{37}$$

$$B_{13}^{[k]} = -B_{31}^{[k]} = \nu h^{[k]} \tag{38}$$

$$B_{14}^{[k]} = -B_{41}^{[k]} = \nu h^{[k]}R^{[k]} \tag{39}$$

$$B_{21}^{[k]} = (1-\nu)\frac{\left(h^{[k]}\right)^2}{12}\left(mh^{[k]} + 3\left(\frac{dR_o}{dx}\right)^{[k]}\right) \tag{40}$$

$$\begin{aligned} B_{21}^{[k]} = &-\mu h^{[k]}R^{[k]} + (1-\nu)\frac{\left(h^{[k]}\right)^3}{24}2m^2R^{[k]} \\ &+ m(1-\nu)\frac{\left(h^{[k]}\right)^2}{24}\left(6R^{[k]} + h^{[k]}\right)\left(\frac{dR_o}{dx}\right)^{[k]} \end{aligned} \tag{41}$$

$$B_{23}^{[k]} = -m\mu h^{[k]}R^{[k]} \tag{42}$$

$$B_{24}^{[k]} = -\frac{\left(h^{[k]}\right)^2}{12}\left[m(\mu-2\nu)h^{[k]} - 6\nu\left(\frac{dR_o}{dx}\right)^{[k]}\right] \tag{43}$$

$$B_{32} = \mu\left[mh^{[k]}R^{[k]} + \left(R^{[k]} + \frac{h^{[k]}}{2}\right)\left(\frac{dR_o}{dx}\right)^{[k]}\right] \tag{44}$$

$$\begin{aligned} B_{34}^{[k]} = B_{43}^{[k]} = &-\left(h^{[k]} - (1-\nu)\alpha^{[k]}R^{[k]}\right) \\ &+ \frac{\mu\left(h^{[k]}\right)^2}{12}\left[m^2\left(h^{[k]}\right) - 3m\left(\frac{dR_o}{dx}\right)^{[k]}\right] \end{aligned} \tag{45}$$

$$B_{42}^{[k]} = \frac{\left(h^{[k]}\right)^2}{12}\left(m(\mu-2\nu)h^{[k]} + 3\mu\left(\frac{dR_o}{dx}\right)^{[k]}\right) \tag{46}$$

$$\begin{aligned} B_{44}^{[k]} = &2m^2\mu\frac{\left(h^{[k]}\right)^3}{24}R^{[k]} - (1-\nu)\alpha^{[k]}\left(R^{[k]}\right)^2 \\ &+ m\mu\frac{\left(h^{[k]}\right)^2}{24}\left(6R^{[k]} + h^{[k]}\right)\left(\frac{dR_o}{dx}\right)^{[k]} \end{aligned} \tag{47}$$

The result of the determinant above is a six-order polynomial, which is a function of m, the solution of which is a 6-eigenvalue m_i. The eigenvalues are 3 pairs of conjugated roots. Substituting the calculated eigenvalues in the following equation, the corresponding eigenvectors are obtained

$$\left[m^2[B_1]^{[k]} + m[B_2]^{[k]} + [B_3]^{[k]}\right]\{V\}^{[k]} = 0 \tag{48}$$

Therefore, the homogeneous solution is

$$\{y\}_h^{[k]} = \sum_{i=1}^{6} C_i^{[k]} \{V\}_i^{[k]} e^{m_i^{[k]} x} \tag{49}$$

The particular solution is obtained as follows

$$\{y\}_p^{[k]} = \left[[B_3]^{[k]} \right]^{-1} \{F\}^{[k]} \tag{50}$$

Therefore, the total solution is

$$\{y\}^{[k]} = \sum_{i=1}^{6} C_i \{V\}_i^{[k]} e^{m_i^{[k]} x} + \left[[B_3]^{[k]} \right]^{-1} \{F\}^{[k]} \tag{51}$$

In general, the problem for each disk consists of 8 unknown values of C_i. The elastic solution is completed by the application of the boundary and continuity conditions.

4 Boundary and continuity conditions

Using SDT, it could be assumed that the cylinder has boundary conditions other than free–free ends. The clamped–clamped (fixed–fixed) boundary is straightforward and implies that the ends of the cylinder are restrained in all coordinate directions and even with that the plane along the edge of the cross-section is assumed not to rotate as opposed to a line tangent to the mid-surface of the shell as in thin shell theories. Simple support end conditions can be given a variety of interpretations. Classically, a simple support boundary condition is characterized with a hinge (ball and socket in three dimensions) or roller if motion is not restrained in all directions [1]. In Table 1 the details of boundary condition for the rotating cylindrical shell are presented. (Table 1)

Table 1 Boundary conditions for each end of cylindrical shell

Direction	Clamped supported	Simply supported	Free end
x	$u = 0$ $\phi = 0$	$u = 0$ $M_x = 0$	$N_x = 0$ $M_x = 0$
z	$w = 0$ $\psi = 0$	$w = 0$ $M_{xs} = 0$	$Q_x = 0$ $M_{xs} = 0$

In this work, two end edges of the cylinder with variable thickness are assumed to be clamped supported. Because of continuity and homogeneity of the cylinder, at the boundary between the two layers, forces, stresses and displacements must be continuous. Given that shear deformation theory applied is an approximation of one order and also all equations related to the stresses include the first derivatives of displacement, the continuity conditions are as follows

$$\begin{Bmatrix} U_x^{[k-1]}(x,z) \\ U_z^{[k-1]}(x,z) \end{Bmatrix}_{x=x^{[k-1]}+\frac{t}{2}} = \begin{Bmatrix} U_x^{[k]}(x,z) \\ U_z^{[k]}(x,z) \end{Bmatrix}_{x=x^{[k]}-\frac{t}{2}} \tag{52}$$

$$\begin{Bmatrix} U_x^{[k]}(x,z) \\ U_z^{[k]}(x,z) \end{Bmatrix}_{x=x^{[k]}+\frac{t}{2}} = \begin{Bmatrix} U_x^{[k+1]}(x,z) \\ U_z^{[k+1]}(x,z) \end{Bmatrix}_{x=x^{[k+1]}-\frac{t}{2}} \tag{53}$$

and

$$\begin{Bmatrix} \dfrac{dU_x^{[k-1]}(x,z)}{dx} \\ \dfrac{dU_z^{[k-1]}(x,z)}{dx} \end{Bmatrix}_{x=x^{[k-1]}+\frac{t}{2}} = \begin{Bmatrix} \dfrac{dU_x^{[k]}(x,z)}{dx} \\ \dfrac{dU_z^{[k]}(x,z)}{dx} \end{Bmatrix}_{x=x^{[k]}-\frac{t}{2}} \tag{54}$$

$$\begin{Bmatrix} \dfrac{dU_x^{[k]}(x,z)}{dx} \\ \dfrac{dU_z^{[k]}(x,z)}{dx} \end{Bmatrix}_{x=x^{[k]}+\frac{t}{2}} = \begin{Bmatrix} \dfrac{dU_x^{[k+1]}(x,z)}{dx} \\ \dfrac{dU_z^{[k+1]}(x,z)}{dx} \end{Bmatrix}_{x=x^{[k+1]}-\frac{t}{2}} \tag{55}$$

Given the continuity conditions, in terms of z, 8 equations are obtained. In general, if the cylinder with variable thickness is divided into n disk layers, 8 ($n_d - 1$) equations are obtained. Using the 8 equations of the boundary condition, 8 n_d equations are obtained. The solution of these equations yields 8 n_d unknown constants.

5 Results and discussion

A cylindrical shell with r_i = 40 mm, a = 20 mm, b = 10 mm, and L = 400 mm is considered in this paper. For analytical and numerical results the properties used are E = 200 GPa and ν = 0,3 . The thick cylindrical shell with variable thickness has clamped-clamped boundary conditions. The internal pressure applied at the $x = 0$ and $x = L$ is P_1 = 40 MPa and P_2 =100MPa respectively. The thick cylinder rotates with ω = 1000 rad/s. The results are presented in a non-dimensional form. Displacement is normalized by dividing to the internal radii. In order to normalize stresses, we define the mean internal pressure parameter as follows:

$$\bar{P} = \frac{P_1 + P_2}{2} \tag{56}$$

Figure 2 illustrates a valid range for using disk layers in calculating the radial displacement and tangential stress.

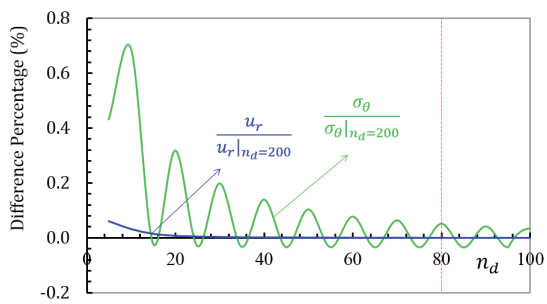

Fig. 5 Effect of the number of disk layers on the radial displacement and tangential stress (m_g = 2, m_p = 2)

It could be observed that if the number of disk layers is more than 40 disks, there will be no significant effect on radial displacement. But the validity range of the tangential stress is lesser than the radial displacement. In other words, one must analyse the cylinder with variable thickness using greater disk layer for determining tangential stress. However, the error of using 80 disk layer in tangential stress calculation is about 0.1%. In the problem in question 80 disks are used.

In order to show the effectiveness and accuracy of the approach suggested here, a comparison between responses of the present theories and FEM can be made. The cylinder with non-uniform thickness is modeled, using a commercial finite element code. An axisymmetric element is applied to represent the cylinder.

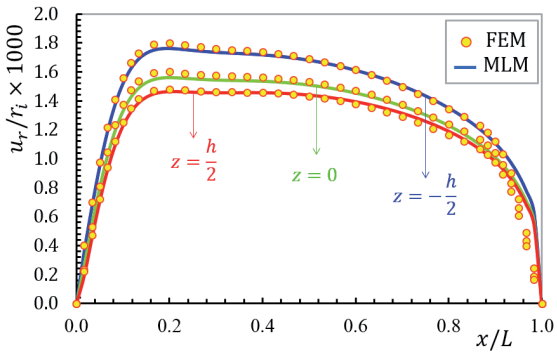

Fig. 6 Normalized radial displacement distribution in different layers ($m_g = 1$, $m_p = 2$)

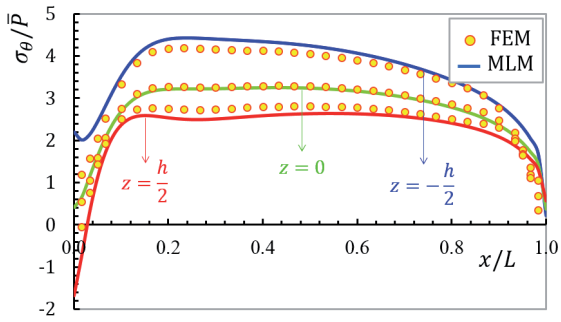

Fig. 7 Normalized tangential stress distribution in different layers ($m_g = 1$, $m_p = 2$)

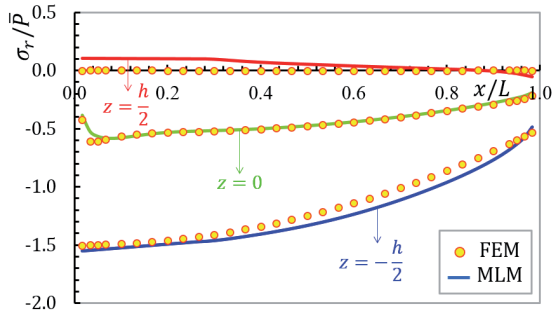

Fig. 8 Normalized radial stress distribution in different layers ($m_g = 1$, $m_p = 2$)

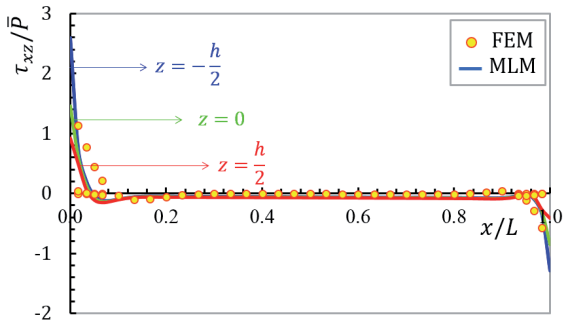

Fig. 9 Normalized shear stress distribution in different layers ($m_g = 1$, $m_p = 2$)

In Figures 6-9, displacement and stress distributions obtained, using MLM, are compared with the solutions of FEM and are presented in the form of graphs. It can be seen that this solution is in good agreement with verified FEM results.

The effects of angular velocity ω on the distribution of the stresses and radial displacement are presented in Figs. 10 and 11. From these figures it is clear that radial displacement and tangential stress rise with increases in angular velocity. In addition, for the angular speed less than 1000 rad/s, the centrifugal force is less effective than the internal pressure.

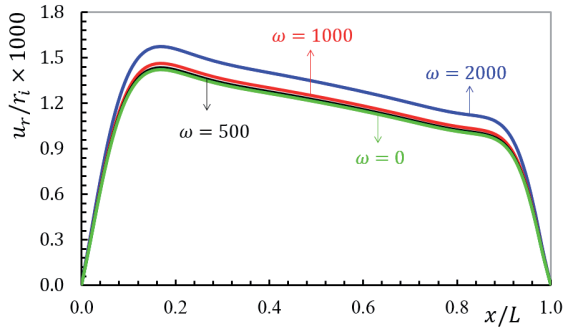

Fig. 10 Normalized radial displacement subjected to various angular velocities ($m_g = 1$, $m_p = 0$)

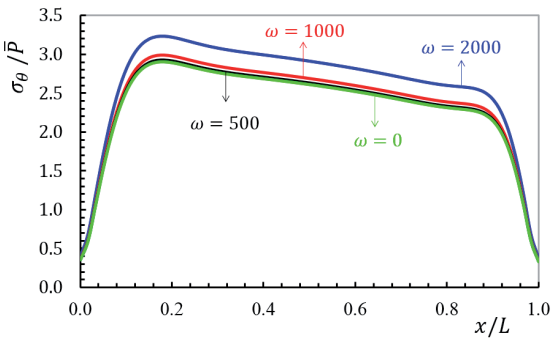

Fig. 11 Normalized tangential stress subjected to various angular velocities ($m_g = 2$, $m_p = 2$)

The influences of profile function on the distribution of displacement and stresses are examined in Figs. 12-13. It is evident that the radial displacement and tangential stress decreases with the increase in the geometry parameter.

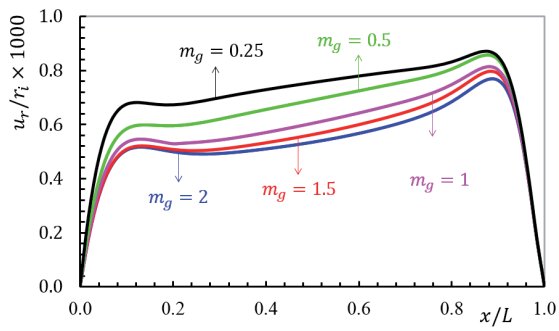

Fig. 12 Normalized radial displacement along the length subjected to different thickness profiles ($m_p = 0$)

The tangential stress at any point of the cylinder with convex thickness profile is smallest in comparison with other thickness profiles, i.e. linear or concave. It is noted that the cylinder with convex thickness profile have smaller radial displacement compared to the cylinder with linear or concave profiles. It can be seen that the maximum tangential stress for the cylinder with any thickness profiles occurred at the same position.

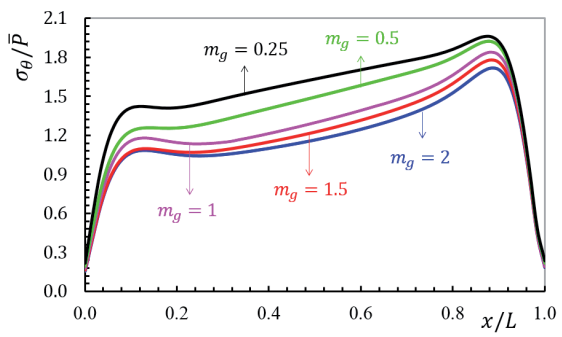

Fig. 13 Geometry Normalized tangential stress along the length subjected to different thickness profiles ($m_p = 0$)

The results of the rotating cylinder are presented to study the impact of the non-uniformity pressure function on the results. For this purpose, the distribution of pressure for different values of m could be seen in Fig. 14. Figure 14 shows that a linear pressure distribution can be obtained by setting $m_p = 1$. The pressure profile is concave if $m_p < 1$ and it is convex if $m_p > 1$.

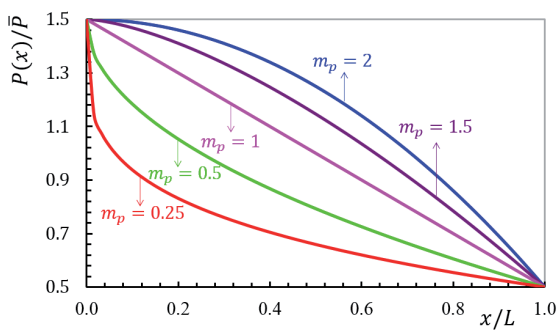

Fig. 14 Axial distribution of non-dimensional inner pressure

Figures 15 and 16 indicate that radial displacement and tangential stress rise with increases in non-uniformity pressure constant m_p.

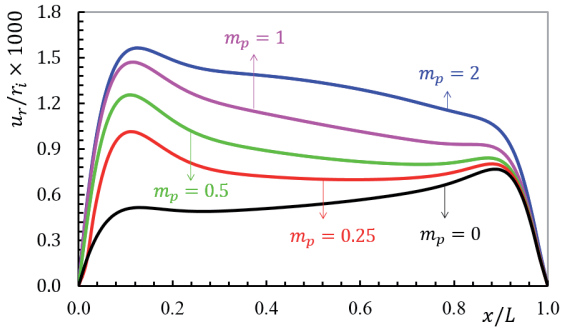

Fig. 15 Geometry of an arbitrary homogenous disk layer

Moreover it could be observed that the radial displacement and tangential stress distributions change with respect to the internal pressure profile. For example, for convex pressure profile, radial displacement and tangential stress profile at points away from the boundaries are convex.

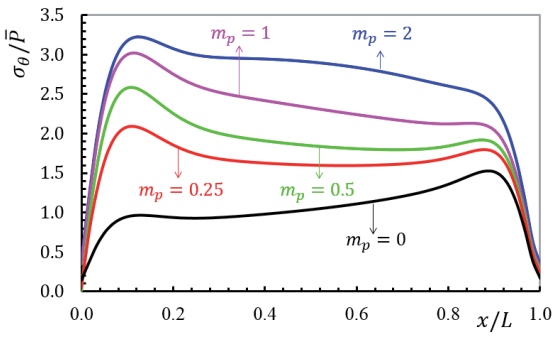

Fig. 16 Geometry of an arbitrary homogenous disk layer

6 Conclusion

In the present study, based on FSDT and elasticity theory, an analysis of thick-walled rotating cylindrical shells with non-uniform variable thickness is presented. Different cases considered under these categories are concave, linear and convex thickness profiles. Elastic solution for the rotating cylinder with clamped-clamped boundary conditions subjected non-uniform internal pressure are obtained by using MLM. The results obtained for stresses and displacements are compared with the solutions carried out through the FEM. Good agreement was found between the results. The effects of the centrifugal force, the geometry parameter (m_g) related to the geometry of the cylinder and internal pressure profiles, on the stresses and displacements are investigated. In summary, the above results reveal that the thickness profile and internal pressure profile have a significant effect on the stress and displacement fields. But the obtained results demonstrate that the centrifugal force effect is negligible. Also, the radial displacement and tangential

stress distributions change with respect to the internal pressure profile. For example, for convex pressure profile, radial displacement and tangential stress profile at points away from the boundaries are convex. It is shown that the tangential stress and radial displacement at any point of the cylinder with convex thickness profile are smallest in comparison with other thickness profiles, i.e. linear or concave.

References

[1] Buchanan, G. R., Yii, C. B. Y. "Effect of Symmetrical Boundary Conditions on the Vibration of Thick Hollow Cylinders." *Applied Acoustics*. 63. pp. 547-566. 2003. DOI: 10.1016/S0003-682X(01)00048-2

[2] Duan, W. H., Koh, C. G. "Axisymmetric Transverse Vibrations of Circular Cylindrical Shells with Variable Thickness." *Journal of Sound and Vibration*. 317. pp. 1035-1041. 2008. DOI: 10.1016/j.jsv.2008.03.069

[3] Eipakchi, H. R., Rahimi, G. H., Khadem, S. E. "Closed form Solution for Displacements of Thick Cylinders with Varying Thickness Subjected to Non-Uniform Internal Pressure." *Structural Engineering and Mechanics*. 16. pp. 731-748. 2003.

[4] Ghannad, M., Nejad, M. Z., Rahimi, G. H. šElastic Solution of Axisymmetric Thick Truncated Conical Shells Based on First-Order Shear Deformation Theory." *Mechanika*. 79. pp. 13-20. 2009.

[5] Ghannad, M., Nejad, M. Z. "Elastic Analysis of Pressurized Thick Hollow Cylindrical Shells with Clamped-Clamped Ends.š *Mechanika*. 85. pp. 11-18. 2010.

[6] Ghannad, M., Rahimi, G. H., Nejad, M. Z. "Determination of Displacements and Stresses in Pressurized Thick Cylindrical Shells with Variable Thickness using Perturbation Technique." *Mechanika*. 18. pp. 14-21. 2012. DOI: 10.5755/j01.mech.18.1.1274

[7] Greenspon, J. E. "Vibration of a Thick-Walled Cylindrical Shell, Comparison of the Exact Theory with Approximate Theories." *Journal of the Acoustical Society of America*. 32. pp. 571-578. 1960. DOI: 10.1121/1.1908148

[8] Kang, J. H., Leissa, A. W. "Three-Dimensional Field Equations of Motion and Energy Functionals for Thick Shells of Revolution with Arbitrary Curvature and Variable Thickness." *Journal of Applied Mechanics-Transactions of the ASME*. 68. pp. 953-954. 2001. DOI: 10.1115/1.1406961

[9] Kang, J. H. "Field Equations, Equations of Motion, And Energy Functionals for Thick Shells of Revolution with Arbitrary Curvature and Variable Thickness from a Three-Dimensional Theory." *Acta Mechanica*. 188. pp. 21-37. 2007. DOI: 10.1007/s00707-006-0391-y

[10] Kang, J. H. "Three-Dimensional Vibration Analysis of Joined Thick Conical-cylindrical Shells of Revolution with Variable Thickness." *Journal of Sound and Vibration*. 331. pp. 4187-4198. 2012. DOI: 10.1016/j.jsv.2012.04.021

[11] Mirsky, I., Hermann, G. "Axially Motions of Thick Cylindrical Shells." *Journal of Applied Mechanics-Transactions of the ASME*. 25. pp. 97-102. 1958.

[12] Naghdi, P. M., Cooper, R. M. "Propagation of Elastic Waves in Cylindrical Shells, Including the Effects of Transverse Shear and Rotary Inertia." *Journal of the Acoustical Society of America*. 29. pp. 56-63. 1956.

[13] Nejad, M. Z., Jabbari, M., Ghannad, M. "A Semi-Analytical Solution for Elastic Analysis of Rotating Thick Cylindrical Shells with Variable Thickness using Disk Form Multilayers." *Scientific World Journa.* 932743. pp. 1-10. 2014. DOI: 10.1155/2014/932743

[14] Nejad, M. Z., Jabbari, M., Ghannad, M. "Elastic Analysis of Axially Functionally Graded Rotating Thick Cylinder with Variable Thickness under Non-Uniform Arbitrarily Pressure Loading." *International Journal of Engineering Science*. 89. pp. 86-99. 2015. DOI: 10.1016/j.ijengsci.2014.12.004

[15] Nejad, M. Z., Jabbari, M., Ghannad, M. "Elastic Analysis of FGM Rotating Thick Truncated Conical Shells with Axially-Varying Properties under Non-Uniform Pressure Loading." *Composite Structures*. 122. pp. 561–569. 2015. DOI: 10.1016/j.compstruct.2014.12.028

[16] Nejad, M. Z., Jabbari, M., Ghannad, M. "Semi-Analytical Solution of Thick Truncated Cones Using Matched Asymptotic Method and Disk Form Multilayers." *Archive of Mechanical Engineering*. 61 (3). pp. 495-513. 2014. DOI: 10.2478/meceng-2014-0029

[17] Nejad, M. Z., Rahimi, G. H., Ghannad, M. "Set Of Field Equations for Thick Shell of Revolution Made Of Functionally Graded Materials in Curvilinear Coordinate System." *Mechanika*. 77. pp. 18-26. 2009.

[18] Vlachoutsis, S. "Shear Correction Factors for Plates and Shells." *International Journal for Numerical Methods in Engineering*. 33. pp. 1537-1552. 1992. DOI: 10.1002/nme.1620330712

[19] Zenkour, A. M. "Stresses in rotating heterogeneous viscoelastic composite cylinders with variable thickness." *Applied Mathematics and Mechanics*. 32 (4). pp. 507-520. 2011. DOI: 10.1007/s10483-011-1434-9